Design and Analysis of Tensile Membrane Structures

+VG Architects

by

Rose Akhavan Tabassi

2B Architectural Engineering

May 2020

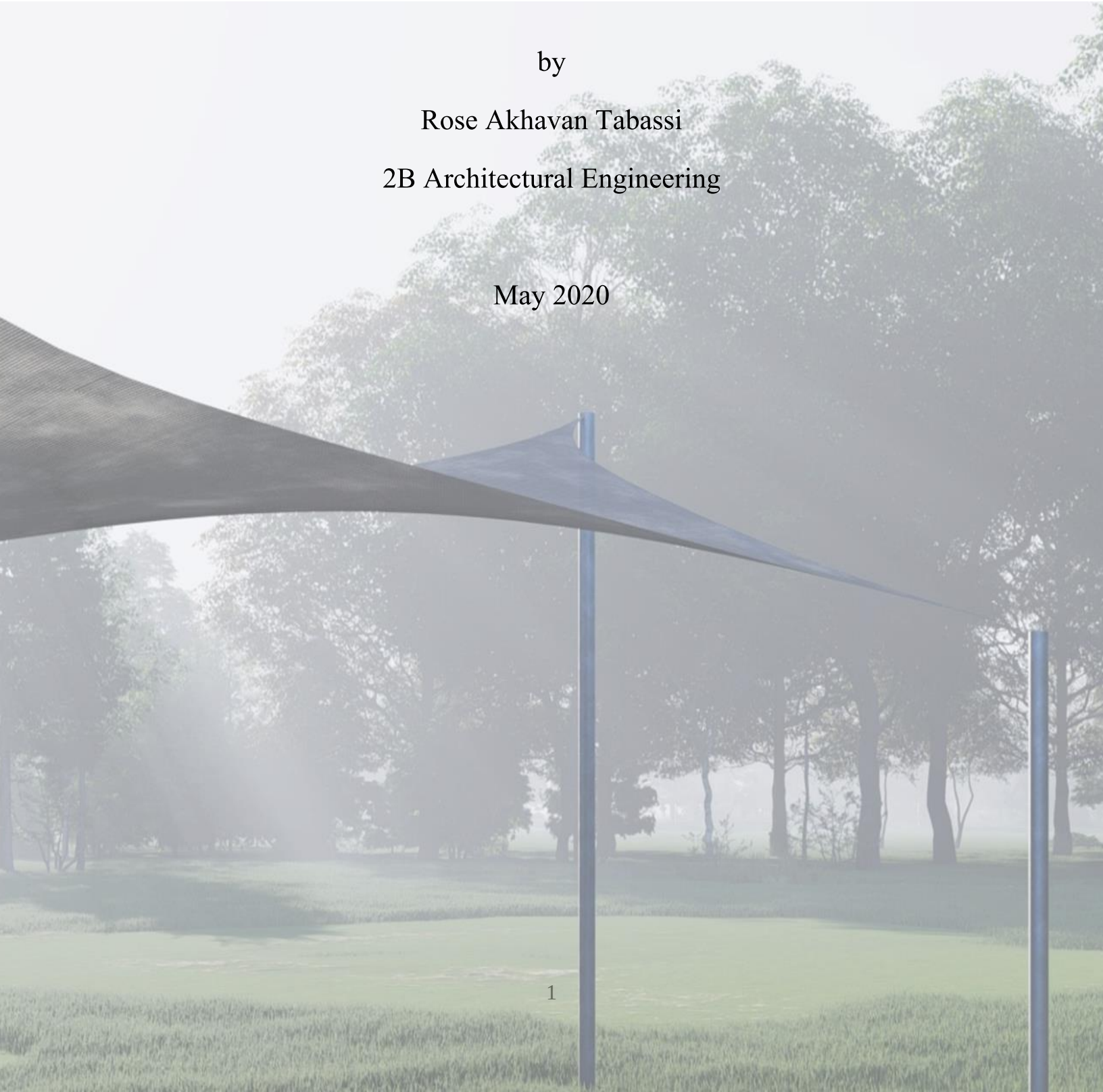

Design and Analysis of Tensile Membrane Structures

+VG Architects

by

Rose Akhavan Tabassi

2B Architectural Engineering

May 2020

Summary

The following report discusses basic properties of cable-membrane structures and the general process for analyzing them. Following that, the procedure for form-finding these geometrically nonlinear structures based on defined prestresses is discussed at a basic level using common numerical approaches. The theory is then applied to a hypar cable-membrane structure using Dlubal RFEM on a structure that is intended on being built by +VG architects. Once the geometric shape of the structure is determined, the objective of this report is to determine the appropriate warp direction for the membrane based on where tensile forces are expected to be the greatest.

Table of Contents

1.0 Introduction 8
1.1 Background 8
1.2 Objective 9
2.0 Theory 10
2.1 Classification of Tension Membranes 10
2.2 Material Properties 12
2.3 Numerical Methods: Force Density 16
2.4 Numerical Methods: Transient Stiffness 19
3.0 Application of Form-finding and Structural Analysis 23
3.1 Application of form-finding 24
3.2 Application of structural analysis with applied loads 29
3.3 Conclusion and Recommendations 32
Works Cited 34

List of Tables

TABLE 1.0: GENERIC PVC MEMBRANE MATERIAL PROPERTIES USED FOR ANALYSIS 15

TABLE 2.0: ISOTROPIC LINEAR-ELASTIC STEEL CABLE MATERIAL PROPERTIES BY PFEIFER 16

List of Figures

FIGURE 1: GROUND FLOOR PLAN OF OVERHEAD HYPAR SHADES TO BE BUILT FOR THE CLIENT 9

FIGURE 2: HEM SLEEVE WITH ROPE INSIDE (MODIFIED FROM SEIDEL [2]) 10

FIGURE 3: DIAGRAM OF CURVATURE CLASSIFICATIONS 11

FIGURE 4: WEFT AND WARP DIRECTIONS OF A WEAVE BY LEWIS [1] 13

FIGURE 5: LOCK-STITCH KNITTED HPDE COMMERCIAL 95 340 MEMBRANE BY GALE PACIFIC IN THE COLOUR 'GUN METAL' (MODIFIED BRIGHTNESS FOR VISIBILITY) 14

FIGURE 6: ISOLATED NODE FROM A SURFACE CABLE NET 16

FIGURE 7: TRANSIENT STIFFNESS ITERATION PROCEDURE WITH THE ASSUMPTION OF LINEAR BEHAVIOUR 20

FIGURE 8: IN PROGRESS (A) PLAN AND (B) ELEVATION OF HYPAR CABLE-MEMBRANES THAT ARE ANALYZED IN THIS REPORT. DEVELOPABLE DRAWINGS ARE UNDER DEVELOPMENT BY ENGINEERS. 23

FIGURE 9: DLUBAL (A) INITIAL ASSUMED SHAPE AND (B) FORM-FINDING RESULT WITH 10% TARGET CABLE RELATIVE SAG AND 1 KN/M WARP AND WEFT MEMBRANE PRESTRESS. 25

FIGURE 10: GLOBAL DEFORMATIONS IN MEMBRANE AT FORM-FINDING STAGE 26

FIGURE 11: BASIC PRINCIPLE INTERNAL FORCES IN THE MEMBRANE N_X (LEFT) AND N_Y (RIGHT) 27

FIGURE 12: AXIAL TENSION FORCES WITHIN THE CABLE 27

FIGURE 13: SAMPLE AXIAL TENSION FORCE FOR A SMALL (A) AND LONG (B) LENGTH BOUNDARY CABLE 28

FIGURE 14: SURFACE INCLINATION OF THE CABLE-MEMBRANE 29

FIGURE 15: EXAGGERATED GRAPHIC OF DEFLECTION FOR SELF-WEIGHT 30

FIGURE 16: GLOBAL DEFORMATION BASED ON 0.240 KN/M^2 LIVE LOAD REQUIREMENT BY ASCE 7 31

FIGURE 17: TRAJECTORY OF PRINCIPLE INTERNAL FORCE N_1 AND N_2 BASED ON 0.240 KN/M^2 LIVE LOAD REQUIREMENT BY ASCE 7 31

1.0 Introduction

The following section contains the purpose, scope, and background information about the stages performed for the design and analysis of the cable membranes.

1.1 Background

The ability to span a structure in small or large, complex configurations has made tension structures a growing trend. Multitudes of various membrane textiles have been developed to permit greater structural capabilities and achieve desired aesthetics. However, the behaviour of tensile membranes is still complex and can be unpredictable. Even if the materials used behave linear elastically such as steel cables, the structure will still be geometrically non-linear for most cases except when prestress values are set exceptionally high. Therefore, unlike conventional structures that rely on 'linear' analysis, tensile membranes require a close collaboration between the engineer and architect because both disciplines must understand that changes in the tension field will affect the geometrical shape of the membrane. They must cooperate to obtain appropriate seaming between fabrics, achieve the right amount of shade or transparency, and ensure adequate structural support.

The first step for designing a tensile membrane is determining the surface shape of the membrane that is defined by the boundaries. Most membranes have a complex geometry that cannot be easily identified with a simple mathematical function. As a result, an iterative form-finding process was undertaken to determine the initial topography of the hypar structures. The resulting form-finding geometry was used to perform basic structural analysis with Dlubal RFEM software.

1.2 Objective

The objective of this report is to determine where tensile forces are greatest in cable-membrane ‘A’ in figure 1 and to use this information to select an optimal warp orientation for the membrane to carry these forces. The orientation of the warp can have a significant impact on the stresses the membrane experiences and can help avoid wrinkling in the fabric.

It is important to note that the scope of work performed for +VG Architects was limited to the form-finding of four hypar membranes around the exterior of a residential property for graphical rendering purposes only. All structural analysis with Dlubal RFEM software was done independently and used solely for this report as drawings and specifications from the engineers are still under development. Therefore, patterns, fabric cuts, connections to supports, and the treatment of seams are not discussed in this report and for simplicity the membrane is assumed one continuous piece. All analysis presented is focused on the cable membrane.

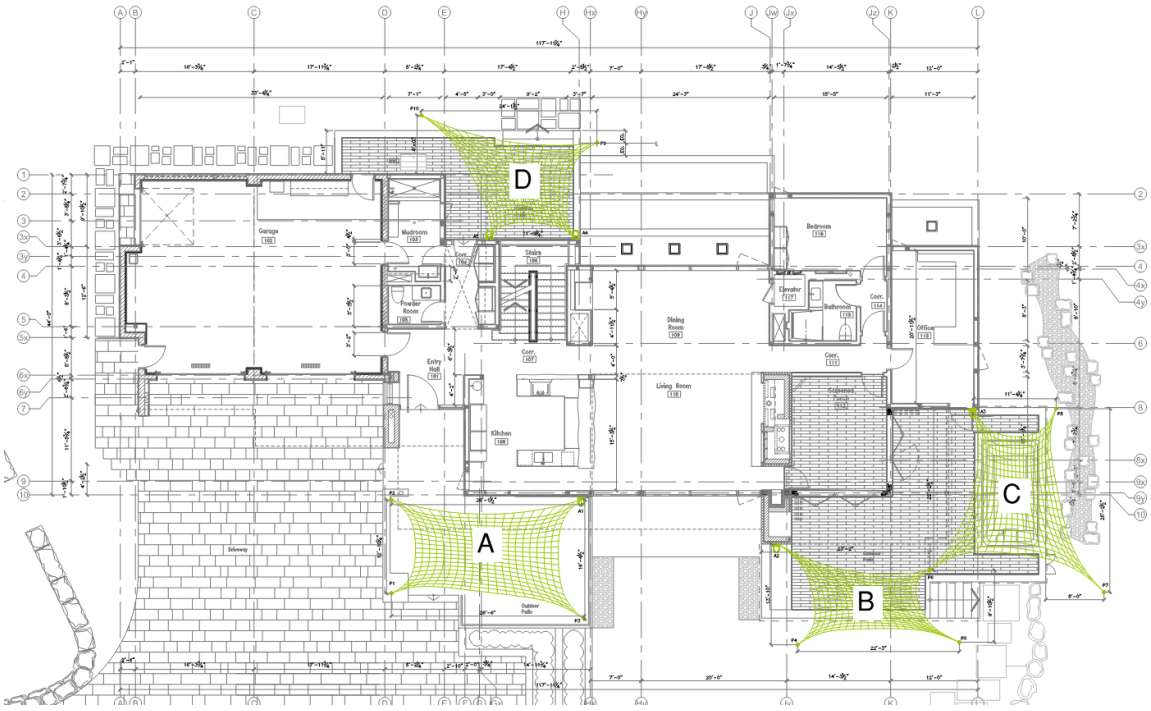

Figure 1: Ground floor plan of overhead hypar shades to be built for the client

2.0 Theory

The form-finding of tensile membranes is a critical step done prior to any further structural analysis. It is the process for achieving the cable bounded membrane in static equilibrium with only its assigned prestresses and no dead or external loads applied [1]. The process is a good sanity check to ensure prestresses are close to what was defined and that certain elements are not at risk of being overstressed before proceeding to structural analysis. The following sections will address some properties for cable membranes, common numerical approaches to form-finding, and an applied result from Dlubal RFEM software.

2.1 Classification of Tension Membranes

There are many different types of tension membranes that use cables; the main classifications are cable nets, pneumatic structures, and boundary tensioned membranes [1]. The term ‘cable membrane’ is used throughout this report to refer to boundary tensioned membranes, which as the name suggests, are membranes bounded by cables along the perimeter. These cables are usually fit into sleeves for smaller structures as in the case of this residential project and later mechanically tensioned onsite (fig. 2).

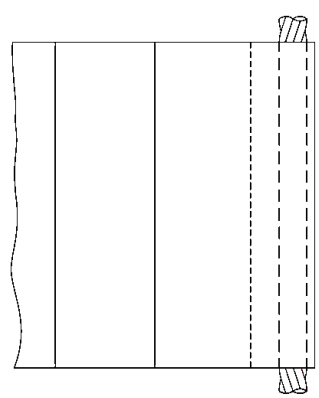

Figure 2: Hem sleeve with rope inside (modified from Seidel [2])

Cable membranes can further be classified according to curvature: single or double curvature. Unlike single curvatures, double curvatures cannot be converted to a flat surface making them considered non-developable [3]. Double curvatures can be classified further based on the signs of their principle curvatures which measure how the surface bends. When the signs of principle radii are equal a synclastic dome takes shape, however when the signs are opposite the shape is anticlastic. Clearly, a hypar structure is anticlastic (fig. 3).

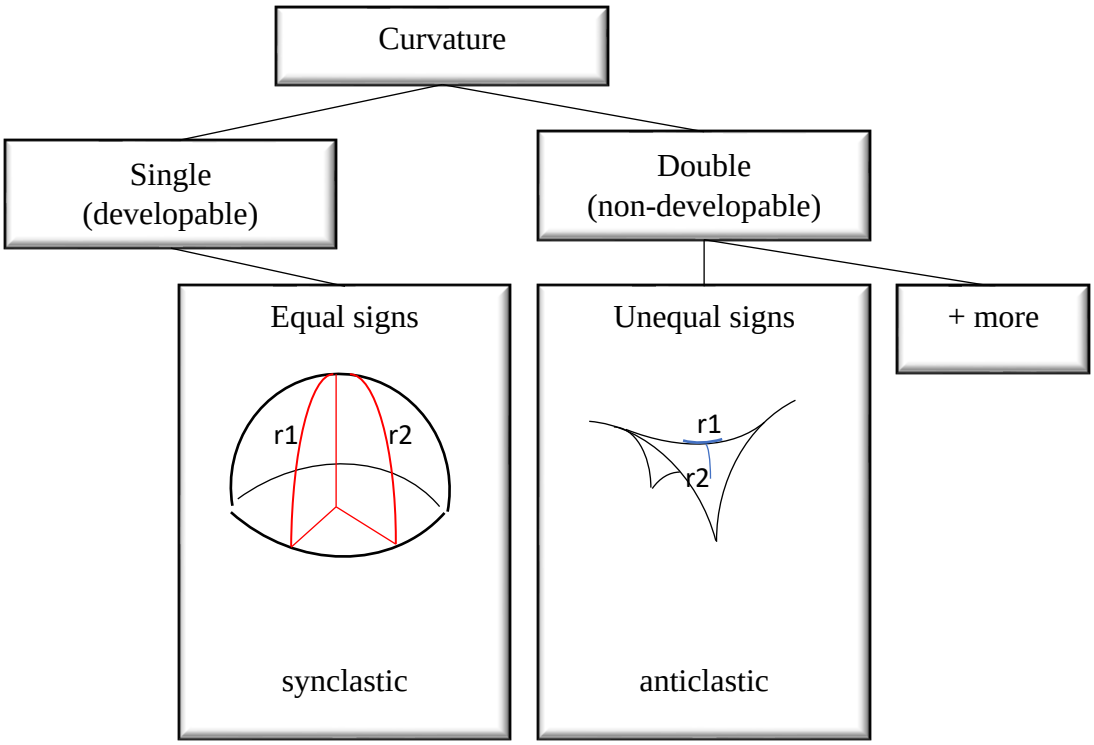

Figure 3: Diagram of curvature classifications

The unequal signs in radii curvatures allows hypar shapes to satisfy equilibrium more easily without the need for external forces. Equation 1.0 demonstrates the relationship between tension forces T_1 and T_2 in their principles directions of r_1 and r_2 for equilibrium normal to a surface piece [3].

$$\frac{T_1}{r_1} + \frac{T_2}{r_2} = P \tag{1.0}$$

For the case of hypar structures where the external force, P, is zero, equilibrium must be satisfied with unequal signs in the radii of principal curvatures since internal tension forces T_1 and T_2 are greater than zero:

$$\frac{T_1}{r_1} = -\frac{T_2}{r_2} \tag{1.0}$$

An external force greater than zero corresponds to pneumatic structures which are pressurized with internal air pressure. This finding explains why hypar shades are ubiquitous and relatively easier to reproduce.

2.2 Material Properties

Membranes are considered to have negligible bending, shear, and compressive stiffness because of their load path sensitivity to applied loads [4]. Therefore, an important process when designing and erecting membranes is prestressing to help increase the stiffness, avoid wrinkling, ponding, and to provide the structure better stability with wind loads. However, prestress levels must also be kept low enough to prevent loss of tension during the lifespan of the structure and tearing under the influence of loads. Prestress values must be pre-defined prior to form-finding and structural analysis [5]. Values vary depending on the geometry of the structure, the expected loads it will experience, and the membrane material.

Membrane fabrics can be either isotropic or orthotropic, but currently orthotropic fabrics are more common in markets. Isotropic fabrics exhibit uniform warp and weft elongation under loads and as a result, the longevity of the fibres increases (fig. 4). Orthotropic fabrics are much more susceptible to deterioration as aging of the two directions is less comparable and re-tensioning is more frequently necessary. Additionally, orthotropic membranes require builders to

have higher attention for proper installation of prestresses in the warp and weft to create a balanced system of stresses.

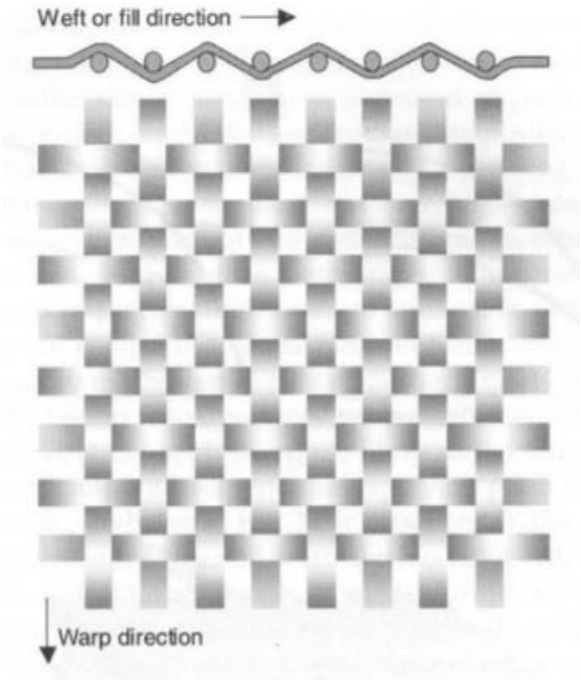

Figure 4: Weft and warp directions of a weave by Lewis [1]

The difference in stiffness between warp and weft fibres can cause greater sagging in the stiffer orientation as more loads can be carried. Typically, the warp direction is classified as the 'stronger' orientation and thus, the membrane is oriented so that the warp can support where principle tensile forces are expected to be greatest.

Due to large snow loads in Canada, the client for this project informed that he would be removing the membranes during the wintertime and the tensile structures are intended more for shading purposes. Therefore, a high density polyethylene membrane (HDPE) was selected by the engineers. This type of fabric is lightweight, widely available, and its relatively low stiffness with wide strain flexibility allows the membrane to stretch steep curvatures for hypar forms [6]. HPDE provides a slight translucency while reflecting light and a good UV stability depending on

the manufacturing method for concentrated pigments. For example, the use of titan dioxide increases UV stability by impeding the penetration of shortwave lengths to fibres [7]. The material does have limitations though such as water permeability because of its open, knit texture; however, this can be advantageous for avoiding ponding and unwanted deflection.

The membrane shown in figure 5 was the fabric selected as per the clients' request. The membrane product is subject to change for a stronger, heavier duty material as form-finding and structural analysis were not done at the time and colours were initially selected for visual purposes.

Figure 5: Lock-stitch knitted HPDE Commercial 95 340 membrane by GALE Pacific in the colour 'Gun Metal' (modified brightness for visibility)

Based on default software properties and common values referenced, Table 1 shows generic material properties for a PVC membrane which will be used instead for form-finding and later structural analysis [1, 4, 7, 8].

Table 1.0: Generic PVC membrane material properties used for analysis

Membrane Property			
Specific Weight	y	5.03	kN/m^3
Modulus of Elasticity (warp)	Ex	49.64	kN/cm^2
*Modulus of Elasticity (weft or fill)	Ey	30.34	kN/cm^2
Shear Modulus, out of plane	G_{yz}	0.01	kN/cm^2
	G_{xz}	0.01	kN/cm^2
Shear Modulus, in membrane plane	G_{xy}	5.00	kN/cm^2
Poisson's Ratio	v_{xy}	0.3	-
	v_{yx}	0.3	-
Constant Thickness	d	1.0	mm

** The modulus of elasticity for the weft will be assumed the same as the warp for isotropic behaviour during form-finding and preliminary structural analysis to determine where tensile stresses are greatest and how the membrane would be best oriented.*

Similarly, for the boundary steel cables, properties were selected based on software material libraries provided by Pfeifer—a German based company with a known reputation in cable membrane construction. Properties including the selected diameter were also compared with similar sized hypar shades [9]. Table 2 shows the material properties for a solid cross-section of an isotropic linear elastic cable.

Table 2: Isotropic linear-elastic steel cable material properties by Pfeifer

Steel Cable Property			
Diameter		12.7	mm
Modulus of Elasticity	E	13000.00	kN/cm^2
Shear Modulus	G	5000.00	kN/cm^2
Poisson's Ratio	v	0.30	-
Specific Weight	y	78.45	kN/m^3
Coefficient of Thermal Expansion	α	1.6000E-05	$1/C^{\circ}$

2.3 Numerical Methods: Force Density

There are many numerical approaches for form-finding membranes; a popular one is the force density method (FDM) which was initially proposed by Linkwitz and Schek to analyze cable net structures for the Munich Olympic games in 1972 [10]. This method can be adapted for the purposes of cable membrane analysis by replacing the surface with a cable net: a process known as surface discretization. A basic explanation of the method is provided by analyzing four cables intersecting at node five (fig. 6).

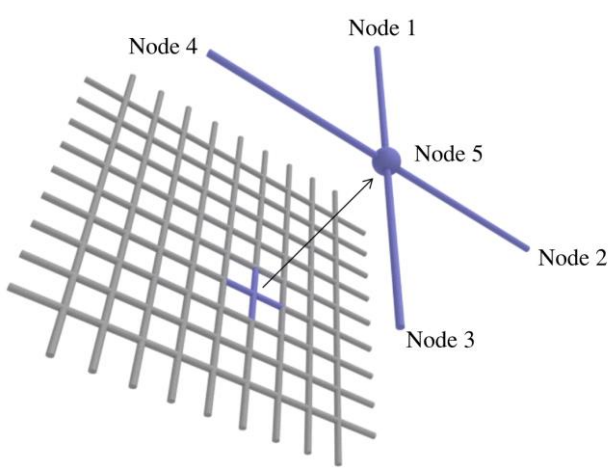

Figure 6: Isolated node from a surface cable net

A system of linear equations for equilibrium in the x,y,z components of node five is developed by multiplying the cable prestressed forces, T_m , with direction cosines:

$$\sum_{m=1}^{4} \left(\frac{x_i - x_k}{L_m}\right)(T_m) = P_x$$

$$\sum_{m=1}^{4} \left(\frac{y_i - y_k}{L_m}\right)(T_m) = P_y \qquad (1.2)$$

$$\sum_{m=1}^{4} \left(\frac{z_i - z_k}{L_m}\right)(T_m) = P_z$$

where in this example with four intersecting cables, m = 1,2,3,4 denotes the cable element; i and k represent the nodal end points of the cable; L_m is the length of the cable element and P is the external load applied at node five. As mentioned earlier, for the purposes of form-finding, external loads including the membrane's own dead weight are not of interest and therefore P can be set to zero. Hence, the expanded equations are:

$$\left(\frac{x_1 - x_5}{L_1}\right)(T_1) + \left(\frac{x_2 - x_5}{L_2}\right)(T_2) + \left(\frac{x_3 - x_5}{L_3}\right)(T_3) + \left(\frac{x_4 - x_5}{L_4}\right)(T_4) = 0$$

$$\left(\frac{y_1 - y_5}{L_1}\right)(T_1) + \left(\frac{y_2 - y_5}{L_2}\right)(T_2) + \left(\frac{y_3 - y_5}{L_3}\right)(T_3) + \left(\frac{y_4 - y_5}{L_4}\right)(T_4) = 0 \qquad (1.3)$$

$$\left(\frac{z_1 - z_5}{L_1}\right)(T_1) + \left(\frac{z_2 - z_5}{L_2}\right)(T_2) + \left(\frac{z_3 - z_5}{L_3}\right)(T_3) + \left(\frac{z_4 - z_5}{L_4}\right)(T_4) = 0$$

The length of the cable element, L_m, poses a challenge because it is a nonlinear function of the nodal coordinates:

$$L_m = \sqrt{(x_k - x_i)^2 + (y_k - y_i)^2 + (z_k - z_i)^2} \qquad (1.4)$$

However, Linkwitz and Schek resolve this problem into linearized equations using the idea of Hooke's law by introducing constant force densities where the ratio of prestress tension to cable length is constant [11]:

$$q_m = \frac{T_m}{L_m} \tag{1.5}$$

Applying this concept to equations 1.3 from earlier simplifies them to the following:

$$\begin{gathered}
(\mathrm{x}_1 - \mathrm{x}_5)(\mathrm{q}_1) + (\mathrm{x}_2 - \mathrm{x}_5)(\mathrm{q}_2) + (\mathrm{x}_3 - \mathrm{x}_5)(\mathrm{q}_3) + (\mathrm{x}_4 - \mathrm{x}_5)(\mathrm{q}_4) = 0 \\
(y_1 - y_5)(\mathrm{q}_1) + (y_2 - y_5)(\mathrm{q}_2) + (y_3 - y_5)(\mathrm{q}_3) + (y_4 - y_5)(\mathrm{q}_4) = 0 \\
(z_1 - z_5)(\mathrm{q}_1) + (z_2 - z_5)(\mathrm{q}_2) + (z_3 - z_5)(\mathrm{q}_3) + (z_4 - z_5)(\mathrm{q}_4) = 0
\end{gathered} \tag{1.6}$$

If coordinates for node one to four are known and values for the force densities are assumed, then equations in 1.3 can be solved using gaussian elimination to determine the final position of node five. According to Lewis, typically a value of one is assigned for non-boundary cable elements and for boundary elements a value inversely proportional to the cable length is set [1, 12]. Thus, the system of equations can indeed be setup to account for the nodal boundary coordinates and remaining cable elements that make up the surface. It is also important to mention that an integral assumption of FDM is that cable elements are straight and both connections between elements and reaction supports are all hinged.

The original FEM presented here does however have a few limitations. In order to maintain a constant ratio of q_m, longer cable lengths must have higher prestresses and smaller cable lengths must have smaller prestresses. Clearly, this not ideal as one of the goals and purposes of form-finding is to ensure that the resulting membrane has prestresses that are close to what was predefined without elements that needlessly have higher stresses at risk of failure during structural analysis. This should not be a problem if elements are the same length, however

with very little constraints imposed on them a vast range of configurations can be obtained that leave the elements susceptible to irregular lengths. As a result, the method has been extended to nonlinear iterations that include additional constraints that only allow uniform rectangular meshing.

2.4 Numerical Methods: Transient Stiffness

This section gives a basic theoretical overview of the transient stiffness method—another numerical method for cable-membrane analysis. This method gained popularity because it draws some parallels to the procedure behind the renown Newton Raphson Method except it is 'vectorized' [1].

In mechanics the displacement δ for a bar of constant load P and cross-sectional area A can be described by the following relationship [13]:

$$\delta = \frac{PL}{AE} \tag{1.7}$$

The equation can be rearranged, and the axial stiffness AE/L can be substituted with K:

$$K\delta = P \tag{1.8}$$

Obviously as the complexity of a system increases with more elements, it is easier to make the parameters above related to global x,y,z axes instead of local element axes if not done so already. As a result, the displacement and external load can be resolved into their x,y,z components as a nodal column vector:

$$\{\delta\} = \begin{matrix} \delta_x \\ \delta_y \\ \delta_z \end{matrix} \tag{1.9}$$

$$\{P\} = \begin{matrix} P_x \\ P_y \\ P_z \end{matrix} \tag{2.0}$$

Likewise, K becomes a global stiffness matrix, $[K]$, that relates the elements. For compatibility, the size of the global stiffness matrix depends on the number of unknowns in the displacement vector. Therefore, the new vectorized equation for the nodes becomes:

$$[K]\{\delta\} = \{P\} \tag{2.1}$$

The equation above cannot be used directly for the analysis of cable-membranes; an inherent assumption of it is that member displacements are small and linearly proportional to the force. As mentioned previously, in the case of cable-membranes the structure is geometrically nonlinear and therefore, iterations are required. The process in figure 7 outlines a method for solving equation 2.1 with the same assumption of linear behaviour by using iterations until equilibrium is reached.

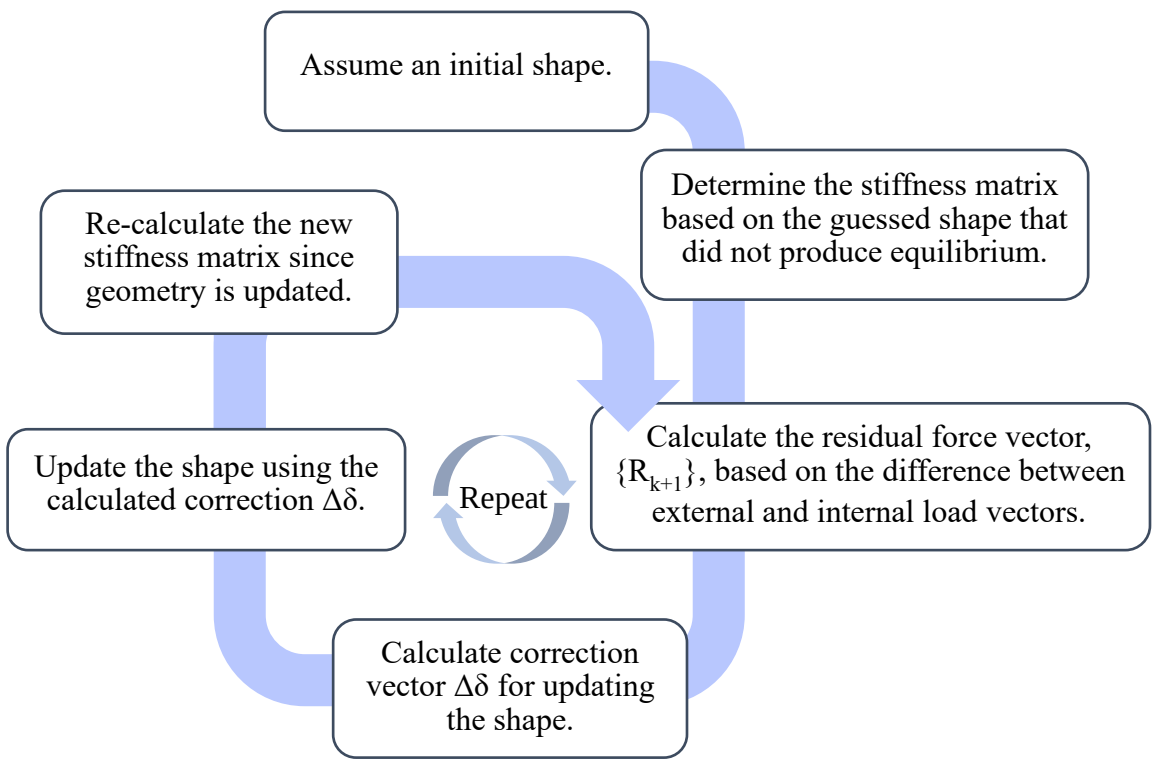

Figure 7: Transient stiffness iteration procedure with the assumption of linear behaviour

The first step for form-finding or static analysis is to assume a shape for the cable-membrane. This shape is denoted as $[x]_k$, where k is the iteration number and the shape is based on its calculated stiffness matrix $[k]_k$. When the shape is first assumed, it will very likely be wrong and not achieve static equilibrium because the internal forces will not cancel out to zero. This excess internal force or difference between external and internal forces is also referred to as the residual $\{R\}$. As a result, a new displacement vector must be calculated to get the assumed shape closer to static equilibrium:

$$\{\delta\}_{k+1} = [k]_k^{-1}\{\Delta R\}_k \tag{2.2}$$

At this step it is imperative that only a small portion $\{\Delta R\}_k$ of the residual is used to maintain the governing linear relationship between force and displacement. The displacement calculated in equation 2.2 can be added to the current geometry $[x]_k$ to determine the new shape:

$$\{x\}_{k+1} = \{x\}_k + \{\delta\}_{k+1} \tag{2.3}$$

When a new shaped is obtained, the stiffness matrix will also change and must be recalculated as $[k]_{k+1}$. Before the iteration starts to repeat again, the internal force vector $\{\tilde{P}\}$ is recalculated to determine if static equilibrium is reached or if there is a residual:

$$[k]_{k+1}\{\delta\}_{k+1} = \{\tilde{P}\}_{k+1} \tag{2.4}$$

Typically, many iterations will be necessary before static equilibrium is achieved since only tiny amounts of the full residual vector are used to ensure linearity in the governing relationships mention earlier. It is also important to not select a $\{\Delta R\}$ too tiny because that may significantly increase the time required to reach convergence or in other words, static equilibrium.

Previously, it was mentioned that the residual $\{R\}$ can either be the excess internal forces in the cable-membrane or an excess difference between external and internal forces. The former

is applicable for form-finding, where the external applied loads including dead weight are not being considered. Meanwhile, the later definition of the residual would be applicable for structural analysis, where applied loads are being considered. In the case of structural analysis, if convergence is not achieved in equation 2.4 then the following residual should be determined for the correction displacement:

$$\{R\}_{k+1} = \{P\} - \{\tilde{P}\}_{k+1} \tag{2.5}$$

For form-finding, one may proceed back to the procedure outlined in equation 2.2, but for the next iteration. Subsequently, the same procedure that was outlined in figure 7 can be followed until static equilibrium is achieved where the residual force approximates close to zero.

The method described above is a start for being able to analyze cable-membranes. The limitations of it are clear: external loads must be trivial with high structural prestresses for iterative, linear behaviour to be acceptable. Geometric stiffness must be accounted to be able to analyze cable-membranes with prestresses at reasonable values. Therefore, the actual stiffness matrix used would consist of two parts:

$$[k] = [k_L] + [k_G] \tag{2.6}$$

where $[k_L]$ is the elastic stiffness and $[k_G]$ is the geometric stiffness. Unlike the elastic stiffness, geometric stiffness does not depend on material properties. Instead, it relies on the length or geometry to change so that tension forces at nodes can update .

Overall, the transient stiffness method is an effective approach to analyzing cable membranes and it is commonly used in form-finding software. The limitations of the method are mostly with ensuring properly conditioned matrices if scripted by one-self. A slight round-off error can lead to major in accuracies in results since the method is iterative [1].

3.0 Application of Form-finding and Structural Analysis

This section applies form-finding and introductory structural analysis to the hypar cable-membrane in figure 8 to determine the objective of this report: locating where tensile forces are greatest in the membrane and selecting an optimal direction for the warp to carry these forces. All analysis presented is done using Dlubal RFEM software.

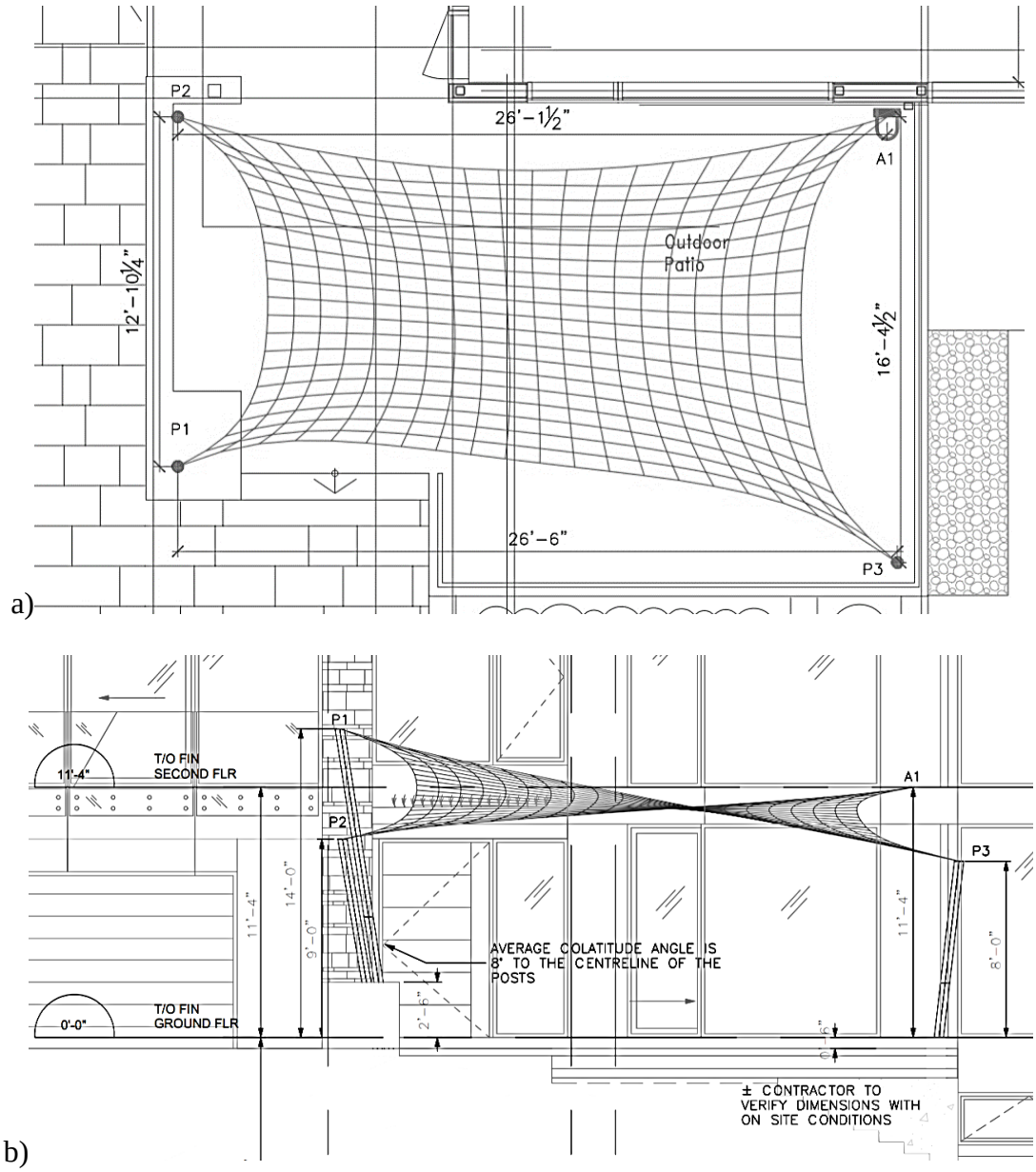

Figure 8: In progress (a) plan and (b) elevation of hypar cable-membranes that are analyzed in this report. Developable drawings are under development by engineers.

Dlubal RFEM is a German-based, comprehensive structural analysis software. The software is comparatively user-friendly with many videos and detailed descriptions on how to properly use its dedicated RF-FORM-FINDING module. The finite element method behind RF-FORM-FINDING is the updated reference strategy (URS) developed by Professor Bletzinger and Professor Ramm [14, 15]. Irrespective of the finite element method used, the general approach for form-finding is consistent: an initial shape is assumed with given prestresses and nonlinear iterations are performed till static equilibrium is approximately reached for the new shape [16]. The word 'approximately' is used because as demonstrated with the Transient Stiffness Method in section 2.4, the tolerances set will usually have an infinitesimally small residual force remaining that is greater than zero, but small enough to approximate the system to equilibrium.

3.1 Application of form-finding

The importance of form-finding prior to structural analysis is to determine the geometry of the hypar membrane and ensure defined prestresses match close to the outputted prestresses. If elements greatly deviate, they may appear overstressed and skew results when trying to locate where tensile forces are greatest in the membrane.

Previously in section 2.2 it was mentioned that the material used for analysis of this hypar membrane is a generic, PVC/polyester fabric. An isotropic prestress of 1.0 kN/m is set for the n_x and n_y of this membrane based off common values reported in literature for PVC fabrics [1,7,8 17,18,19]. For the boundary cables, the appropriate pretension force is set to be determined by the software using a target cable relative sag of 10%. The advantage of using a target sag expressed as a percentage is that it helps ensure that an adequate inward curvature is established at the boundaries of the membrane (fig. 9). Maintaining this curvature is particularly important

for long cable-membranes such as this one because it helps alleviate the fibres from larger stresses [20]. As result, the structure is able retain its geometry more easily. According to Garth Graham, a target catenary curve should usually be between a minimum of 6% to a maximum of 12% [21].

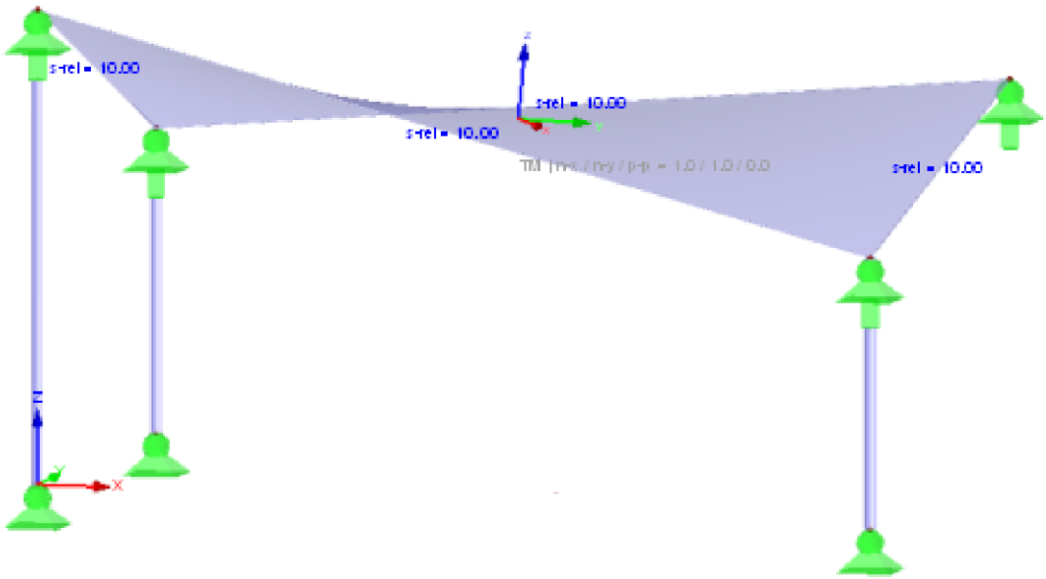

a)

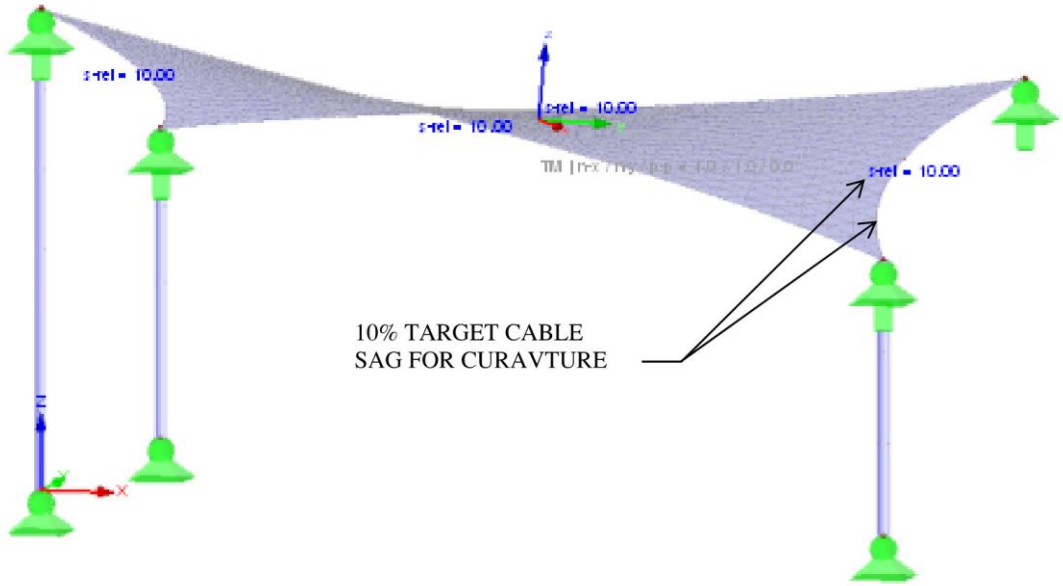

b)

Figure 9: Dlubal (a) initial assumed shape and (b) form-finding result with 10% target cable relative sag and 1 kN/m warp and weft membrane prestress.

The structure shown in figure 9 has pin connections (Fx, Fy, Fz) at each of the four corners of the membrane. One of the pins is an anchor tying back to the existing structure and the rest are vertical poles. The bottom of the poles are fixed supports (Fx, Fy, Fz, Mz), however for the purposes of this report the analysis will be focused on the upper portion of the structure on the behaviour of the membrane.

For the membrane surface, triangular meshing was selected to prevent warping effects that one would see with rectangular elements. Additionally, even though the PVC fabric being used is orthotropic, the weft was temporarily assigned the same modulus of elasticity as the warp because with such an irregular shape it is not necessarily foreseeable which direction the tensile force are going to be exactly greatest. Hence, by using isotropic properties in the beginning, the principle internal forces can be analyzed to determine the general direction where the forces are highest when subjected to loads.

The results show that the deformations in the cable-membrane are largest along the edges and deformations occurred the least towards the centre of the membrane which (fig. 10). This is expected since the cables were prestressed to ensure a 10% inward sag curvature.

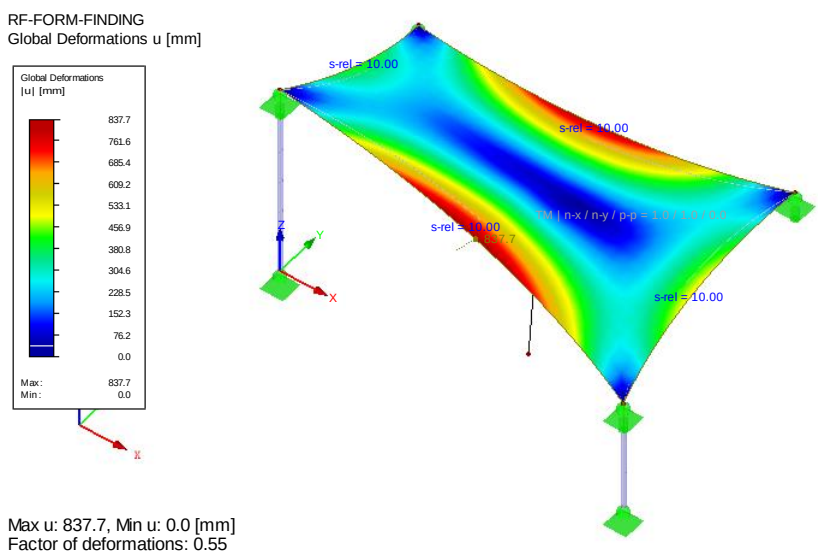

Figure 10: Global deformations in membrane at form-finding stage

The n_x and n_y show the local internal forces in the membrane based on the prestresses defined (fig. 11). The results verify that the prestress forces in the membrane are relatively close to the 1.00 kN/m prestress that was selected earlier since the majority of the model is in the blue range. The max deviation is 1.01 kN/m for both n_x and n_y for only a small region and this occurs near the corner of the membrane.

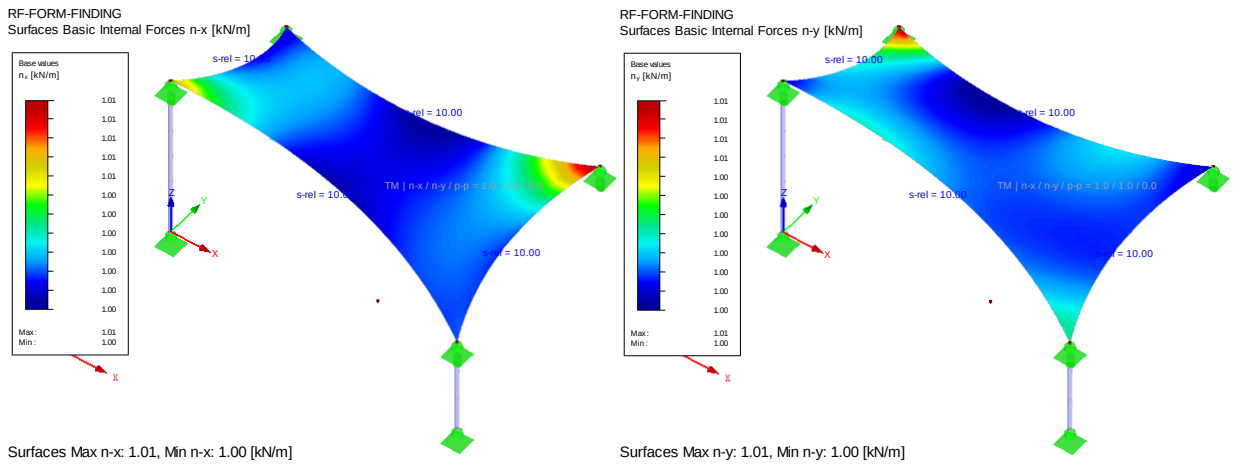

Figure 11: Basic principle internal forces in the membrane n_x (left) and n_y (right)

The cable prestress forces determined by the software based on a 10% target cable sag requirement are shown in figure 12.

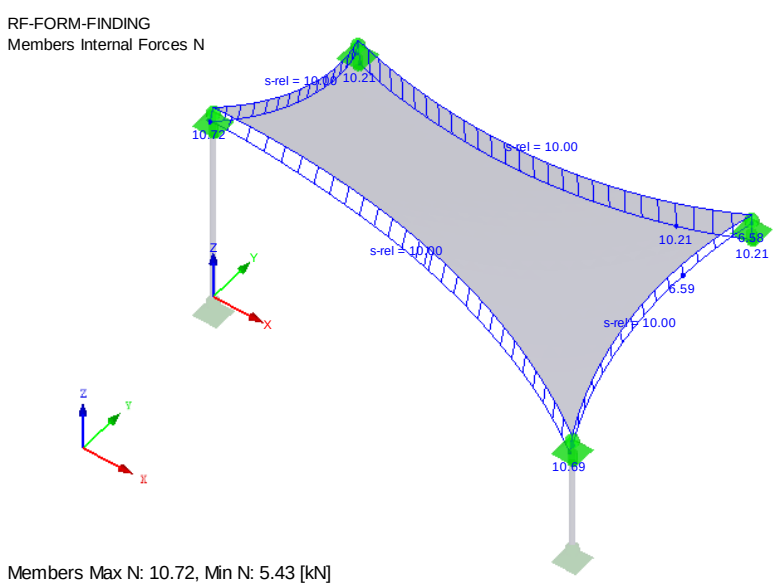

Figure 12: Axial tension forces within the cable

The results show that axial tension force within the cables are around 10-11 kN for the longer edges of the membrane and around 5.5 – 6.5 kN for the shorter width of the membrane. A sample diagram of the internal forces for a short and long cable in figure 13 shows that the axial force is fairly consistent throughout the length of the cable which is inuitive since the cable is expected to carry stress directly and transfer forces tangent to longitudinal axis [22].

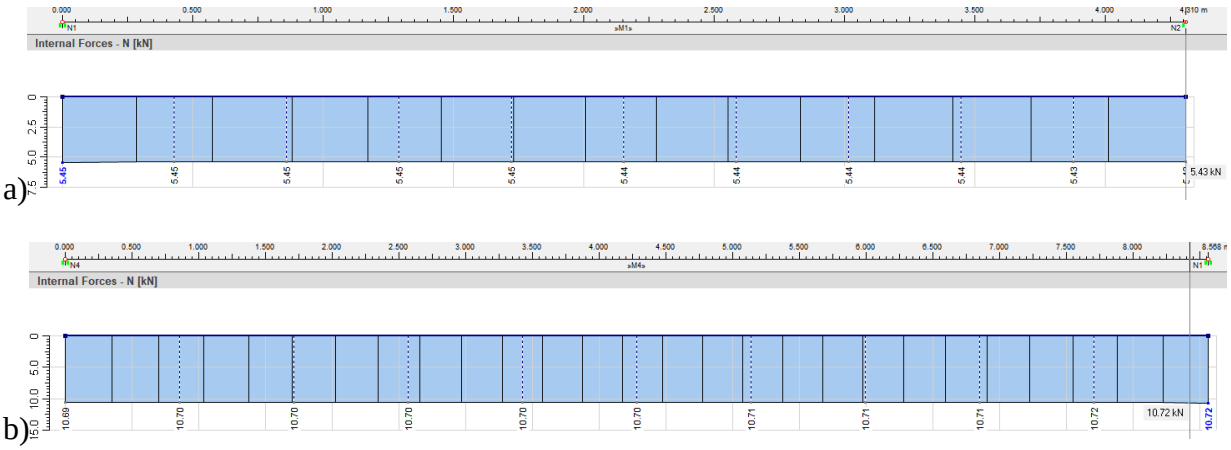

Figure 13: Sample axial tension force for a small (a) and long (b) length boundary cable

Another potentially useful feature that can be extracted during the form-finding phase is the membrane's slope. This information can be used to predict where ponding may occur in the structure and where the membrane may be suceptibile to large deflections from snow and rain loads. For example, the region in dark blue is the flattest area of the membrane and therefore, its lack of double curvature may compromise its ability to withstand loads. Meanwhile, the red regions with high inclination will be able the shed water and snow loads off more easily.

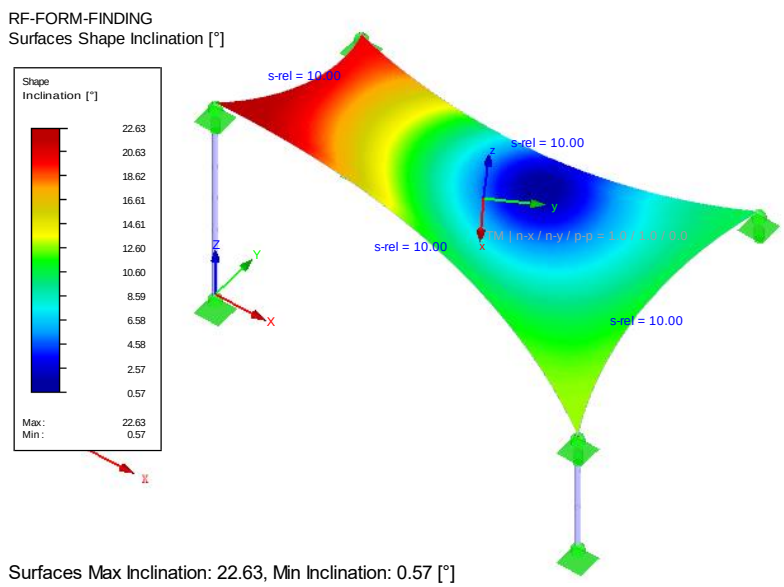

Figure 14: Surface inclination of the cable-membrane

3.2 Application of structural analysis with applied loads

Previously during the form-finding stage the analysis was mostly concerned with geometric results since elastic effects and materiality are not the focus of form-finding. In this section the warp direction for the fabric membrane will be selected based on where the principal internal forces are greatest when the membrane is subjected to applied loads. The loads that will be discussed is the dead load or self-weight of the fabric and live load. The live load that will be applied is based on the 2016, ASCE 7 standard where in table 4.3-1 for fabric canopies, a minimum live load of 5 psf (0.240 kN/m^2) is required to be tested [23]. Wind loads will not be discussed due to the complexity and depth of analysis required, however aeroelastic modelling is an important aspect of analyzing tension membranes to avoid fluttering, resonance, and other unwanted effects. For small structures, extensive field and testing experience is particularly needed to predict behaviour [1]. For big projects and speciality structures, physical modelling and wind tunnel testing may be required.

An exaggerated picture of the expected deflection for self-weight is shown in figure 15. The largest expected deformation under self-weight is only 5.3 mm based on the generic PVC fabric material that was applied with the properties discussed in section 2.2.

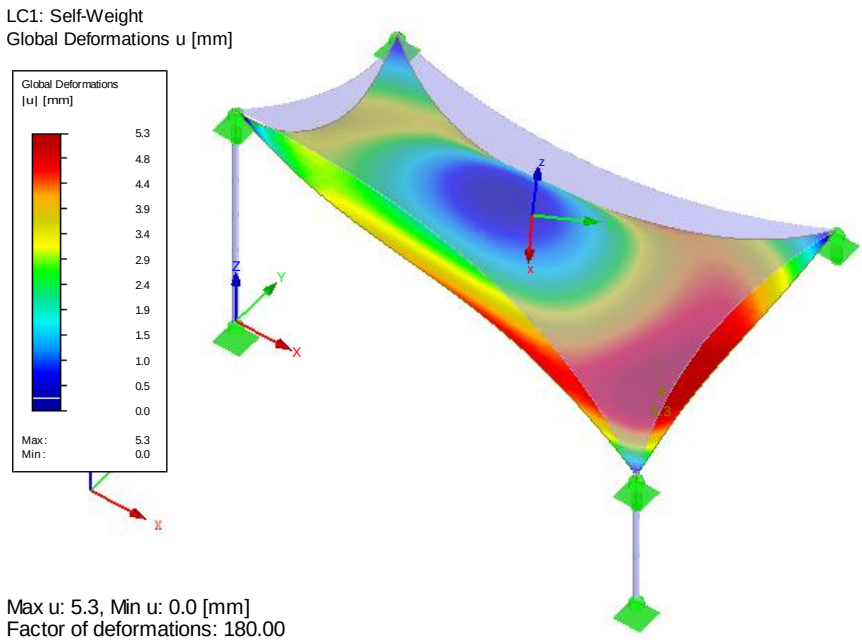

Figure 15: Exaggerated graphic of deflection for self-weight

The next load case is the 0.240 kN/m^2 live load which has a maximum expected deflection of 94 mm (fig. 16). This load was applied globally to the true area in the Z-direction. The region with the largest deformation due to the live load is similar to the region where the largest deformation was seen with self-weight. This indicates that near this particular cable edge additional reinforcement may potentially be necessary if even higher loads are expected to be carried.

In section 3.2 it was discussed that the membrane would be assumed isotropic for form-finding and preliminary structural analysis to be able to better determine where principle internal forces are highest in the membrane. Now that a live load is applied, figure 17 shows the trajectory for the load distribution of principal internal forces n_1 and n_2.

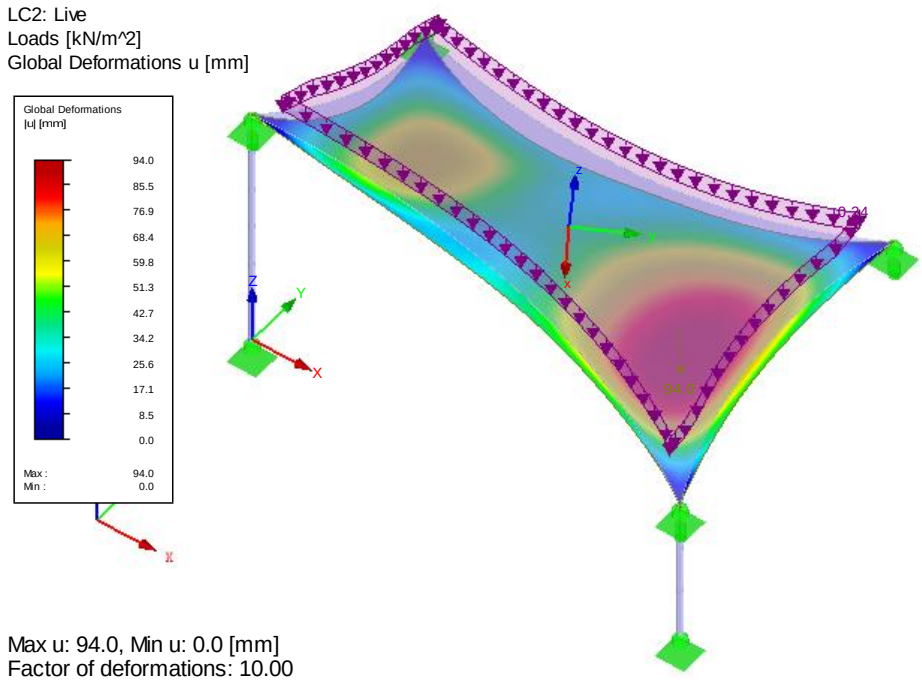

Figure 16: Global deformation based on 0.240 kN/m^2 live load requirement by ASCE 7

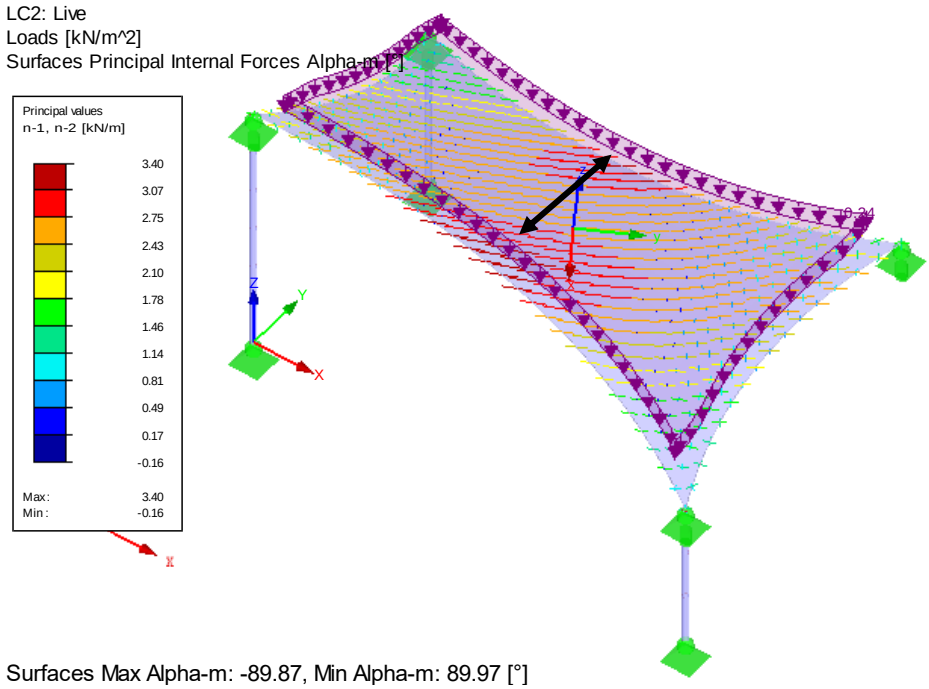

Figure 17: Trajectory of principle internal force n_1 and n_2 based on 0.240 kN/m^2 live load requirement by ASCE 7

Upon close inspection, the trajectory shows that the tensile forces a greatest along the corner to corner of the membrane indicated with a bold black arrow. Hence, the strong axis of the

membrane, the warp, is reoriented to follow suit. An immediate reduction of the internal forces can be seen in figure 18 with the local axes of the membrane reoriented.

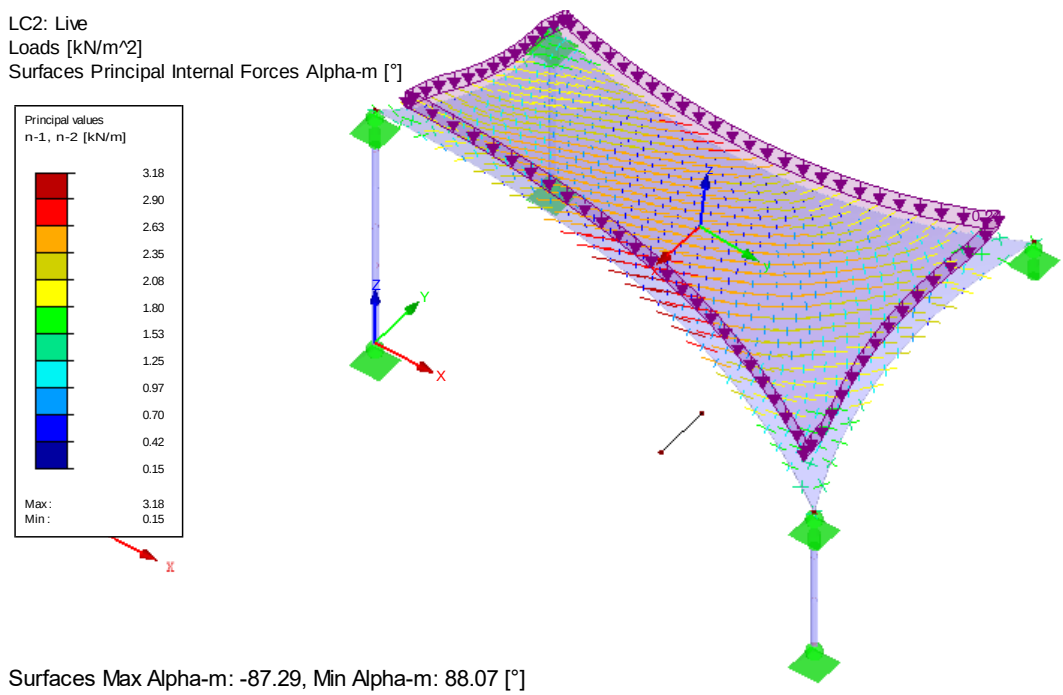

Thus, the modulus of elasticity for the weft of the fabric may now be substituted with its actual value and the remainder of the analysis can be resumed.

3.3 Conclusion and Recommendations

In conclusion, the findings discussed and presented are only an introductory for the analysis of cable-membranes. The complex nonlinear geometric behaviour of these structures requires rigorous evaluation of wind loads, combinations of loads, warping effects in patterning and cutting membranes, seams between fabric rolls, connections, proper pole foundations, and much more. When applicable, using isotropic fabrics is more reliable than orthotropic fabrics to be forgiving of imperfect installation on site and uniform aging in the fabric.

For future studies, the cable-membrane could be analyzed under different loading conditions with different materials to determine which fabrics would not be appropriate for the

intended purposes of this structure. Additionally, the results can be compared with different software and finite element methods to analyze discrepancies and compare the rate of convergence.

Works Cited

[1] W. Lewis, Tension structures. Form and behaviour, Thomas Telford , 2003.

[2] M. Seidel, Tensile Surface Structures: A Practical Guide to Cable and Membrane Construction, Ernst & Sohn, 2009.

[3] B. Topping and P. Ivanyi, Computer Aided Design of Cable Membrane Structures, Saxe-Coburg Publications, 2007.

[4] T. Linthout, "Form-finding and patterning of fabric structures using shape optimization techniques," Universiteit Gent, 2016.

[5] W. Yi and Z. Limei, "Form-finding Analysis of the Tensioned Membrane Structure Considering Cutting Lines," Atlantis Press, 2015.

[6] C. G. Huntington, The Tensioned Fabric Roof, 20004: ASCE Press.

[7] J. Ignasi de Llorens, Fabric Structures in Architecture, Cambridge: Woodhead Publishing Limited, 2015.

[8] M. Euni Son, "The Design and Analysis of Tension Fabric Structures," Massachusetts Institute of Technology, Massachusetts, 2007.

[9] W. Lewis, M. Jones and K. Rushton, "DYNAMIC RELAXATION ANALYSIS OF THE NON-LINEAR STATIC RESPONSE OF PRETENSIONED CABLE ROOFS," Pergamoo Press Ltd., Great Britain, 1983.

[10] P. Broughton and P. Ndumbaro, "The Analysis of Cable and Catenary Structures," Thomas Telford, London, 1994.

[11] P. Gidak and K. Fresl, "Programming the Force Density Method," Seoul, 2012.

[12] W. Lewis, "Computational form-finding methods for fabric structures," ICE Publishing, 2008.

[13] R. Hibbeler, Mechanics, Boston: Pearson, 2017.

[14] K.-U. Bletzinger, J. Linhard and R. Wüchner, "Advanced Numerical Methods for the Form Finding and Patterning of Membrane Structures," Technical University of Munich, Munich.

[15] F. H. Dieringer, "Numerical Methods for the Design and Analysis of Tensile Structures," Technical University of Munich, Munich, 2014.

[16] . R. Lang, "Design and Analysis of Membrane Structures in FEM-Based Software," Anhalt University of Applied Sciences, Faculty of Architecture, Facility Management, and Geo Information, Brno, 2017.

[17] P. Kneen, B. Cahill and P. Lim, "An Introduction to Tension Fabric Structures," 2016. [Online]. Available: http://www.lsaa.org/images/events/LSAA2016/Membrane_Structures_Resource_2016_4xLandscape.pdf.

[18] A. L. Biagini and A. NAVA, "Form-Finding and Mechanical Behaviour of Cable and Membrane Structures," POLITECNICO DI MILAN, School of Civil Environmental and Territorial Engineering, Milan, 2018.

[19] S. PUYSTIENS, . M. VAN CRAENENBROECK, M. MOLLAERT, D. VAN HEMELRIJCK and L. DE LAET, "IMPLEMENTATION OF BENDING ACTIVE ELEMENTS IN KINEMATIC FORM ACTIVE STRUCTURES: DESIGN OF A REPRESENTATIVE CASE STUDY," Elsevier, Brussels, 2015.

[20] C. G. Huntington, "Structures Using Uncurved or Minimally Curved Tensioned Fabric Membranes," 2008.

[21] G. Graham, Interviewee, *Getting the basics right: Installing Architectural shade fabric.* [Interview].

[22] K. M. Leet, C.-M. Uang, J. T. Lanning and A. M. Gilbert, Fundamentals of Structural Analysis, New York: McGraw-Hill, 2018.

[23] C. G. Huntington, Tensile Fabric Structures Design, Analysis, and Construction, Virginia: American Society of Civil Engineers, 2013.